Journal of Catalysis **188,** 375–384 (1999)
Article ID jcat.1999.2664, available online at http://www.idealibrary.com on IDEAL®

Perturbed Angular Correlation Characterization of Indium Species on In/H-ZSM5 Catalysts

E. E. Miró,* L. Gutiérrez,* J. M. Ramallo López,† and F. G. Requejo†,[1]

*INCAPE (CONICET), Fac. Ingeniería Química, UNL, Santa Fe, Argentina; and †TENAES (CONICET), Dep. de Física, Fac. Ciencias Exactas, UNLP, CC/67, 1900 La Plata, Argentina

Received June 7, 1999; accepted August 18, 1999

Silicalite-supported indium catalysts (In/H-ZSM5) were characterized by time differential perturbed angular correlation (PAC) and temperature-programmed reduction (TPR). The presence of different indium species was correlated with activity and selectivity during the NO selective catalytic reduction (SCR) with CH_4 in the presence of excess oxygen. The main species identified on the In/H-ZSM5 surface were In_2O_3 (indium sesquioxide crystals); In^+Z^- and $(InO)^+Z^-$ (different indium species exchanged in the zeolitic matrix); and highly dispersed noncrystalline In oxide species not bonded to the zeolitic matrix. Catalysts that were impregnated and then calcined at 500°C had low activity for the reaction under study, showing the presence of only In_2O_3 and noncrystalline In oxide species. Treatment at 750°C in O_2 or at 500°C in H_2 followed by reoxidation at the same temperature resulted in active catalysts showing an appreciable concentration of $(InO)^+Z^-$ active species. The same active species were formed after indium ion exchange of NH_4-ZSM5 was followed by calcination at 500°C. The PAC technique proved to be a powerful tool for the identification and quantification of indium species present on the surface of an H-ZSM5 support.

Key Words: **In-exchanged H-ZSM5; perturbed angular correlation; indium species; NO_x selective reduction with methane; hyperfine interactions.**

1. INTRODUCTION

The perturbed angular correlation (PAC) technique is a useful characterization tool for catalytic systems as it allows *in situ* studies of dispersed and diluted (as low as ppm) phases on catalysts (1, 2). This technique, by measurement of the local electric field gradient (EFG) at the radioactive probe site, can provide information on the characteristics (coordination, symmetry, distortions, etc.) of the different environments of the radioactive probes, their concentrations, and modifications related to *in situ* conditions. This is possible because of the hyperfine interaction between the nucleus of the probe and the EFG produced by the extranuclear (ion and electronic) charges (3). A brief and clear description of this technique and of the typical equipment setup was published by Vogdt and co-workers (4).

In previous studies (5, 6) we reported that the combined use of laser Raman spectroscopy (LRS) and the PAC technique resulted in a powerful tool for the identification of molybdenum species present on the surface of a silica support. While LRS yields information on the nature of the species formed and on the bond lengths of these species, PAC gives direct information on site structure. Moreover, PAC experiments are a powerful aid to quantify the concentrations of molybdenum species identified by these techniques. Compounds containing molybdenum have the advantage that after neutron irradiation the PAC probe ^{99}Mo is formed from natural ^{98}Mo present in the samples. Thus, the extracted information is reliable since the PAC probe does not introduce an impurity.

In the case of In-supported catalysts, the time differential observations of the perturbed angular correlation of γ rays emitted from radioactive ^{111}In (probe) allowed the characterization of different In sites (and In species). Since the EFG depends on r^{-3} (where r is the distance between the probe and the charge), PAC characterizations are very sensitive to distances, the PAC technique becoming a local-environment characterization technique. Thus, PAC experiments are very appropriate for characterizing species with different local environments and/or short range order (as in the case of species exchanged in zeolites).

It has recently been reported that the selective catalytic reduction of NO_x using methane instead of ammonia proceeds even in the presence of excess oxygen on some metal-exchanged zeolites such as Co ion-exchanged ZSM5 and ferrierite (7, 8), Ga-ion exchanged ZSM5 (9), and In ion-exchanged ZSM5 (10). Of those catalysts, Ga-ZSM5 exhibits an extraordinarily high selectivity of NO_x reduction. However, its activity is strongly suppressed by the presence of water (11). Kikuchi and co-workers (12–14) have recently reported that In-ZSM5 has higher SCR activity in the presence of water than Ga-ZSM5, and that addition of a noble metal such as Pt, Rh, or Ir greatly improves the

[1] To whom correspondence should be addressed. Fax: +54–221–4252006. E-mail: requejo@venus.fisica.unlp.edu.ar.

0021-9517/99 $30.00

water tolerance of the catalyst. It has been suggested that the activity of the In-ZSM5 catalyst for the SCR reaction is due to the presence of $(InO)^+Z^-$ groups (14). We have previously reported the first PAC characterization of this species (15).

In the present work, we report a new series of PAC experiments performed on In/H-ZSM5 catalysts prepared by different methods using ^{111}In as a probe. PAC characterization is combined with X-ray diffraction (XRD), temperature-programmed reduction (TPR), and reaction experiments. The aim of this work is to help elucidate the mechanism of incorporation of indium into the zeolite, the nature of the In species present in the catalysts, and their role in the selective reduction of NO_x with methane in the presence of excess oxygen. It should be pointed out that in this first fundamental PAC study, we have carried out characterizations in a dry atmosphere. Since the water vapor effect is of central concern for the SCR reaction, work is in progress with the aim of *in situ* characterizing this interesting system under both dry and wet reaction conditions.

2. METHODS

a. Catalyst Preparation

A commercial Na-ZSM5 zeolite (Chemie Uetikon, PZ-2/54 Na) with a chemical Si/Al ratio of 26.4, determined by chemical analysis, was the starting material. The ammonium form was prepared by ionic exchange using an aqueous solution of NH_4NO_3 (1 M), with a zeolite/solution ratio of 3 g/liter at reflux temperature (ca. 100°C), for 24 h. The degree of ionic exchange was determined by atomic absorption, being higher than 99% of the ionic exchange capacity (CEC).

Indium was incorporated into the zeolite using two methods:

Sample 1 was prepared by the conventional wet impregnation method, stirring an aqueous solution of $InCl_3$ and NH_4-ZSM5 at 80°C until all water was evaporated, followed by drying in a stove at 120°C for 12 h. After that, the solid was pretreated in a dry oxygen atmosphere by heating up to 500°C at 5°C/min and holding the final temperature for 12 h (standard calcination procedure). Different amounts of $InCl_3$ were used so as to obtain samples with 0.6, 2, 3, and 4 wt% In. The pore volumes of these samples were 0.18, 0.18, 0.16, and 0.11 cm^3/g, respectively, and were measured by nitrogen adsorption at 77 K and at $P/P^0 = 0.5$. These samples are referred to in the text as "impregnated samples" or "S1 samples."

Sample 2 was prepared by the standard ionic exchange method, stirring an aqueous solution of $InCl_3$ (0.003 M) and ammonium-form ZSM5 at 80°C (with reflux) for 24 h, followed by filtering and distilled water washing. After that, the sample was dried in a stove at 120°C and calcined at 500°C for 12 h. In this way, an In-exchanged sample with 1.3 wt% In was obtained.

To perform PAC experiments for both samples, the PAC probe ^{111}In was introduced by adding traces of $^{111}InCl_3$ to the nonradioactive $InCl_3$ solution.

After the standard calcination procedure (500°C), some samples were treated as follows:

Treatment A: calcination for 2 h in oxygen at 750°C.
Treatment B: reduction in hydrogen at 500°C for 2 h.
Treatment C: reoxidation in oxygen at 500°C for 2 h.

It should be noted that, while treatments A and B are performed after the standard calcination procedure, treatment C is performed after treatment B.

b. Reaction Experiments

Steady-state reaction experiments were performed using a single-pass flow reactor made of fused silica with an inside diameter of 5 mm and length of 300 mm, operating at atmospheric pressure. The reacting mixture was obtained by mixing four gas lines independently controlled with mass flow controllers. The details of this apparatus are given elsewhere (16).

The conversions for the selective reduction reaction were calculated in terms of N_2 production as $C_{NO} = 2[N_2]/[NO]$, and for CH_4 as $C_{CH_4} = [CO_x]/[CH_4]$, where $[N_2]$ and $[CO_x]$ are gas-phase concentrations after reaction, and $[NO]$ and $[CH_4]$ are feed concentrations. The carbon balance was always better than 95% and the conversions reported were determined after the steady state was reached (usually after 1 h on stream). The gas blends were analyzed before and after reaction using a Varian 3700 gas chromatograph. Zeolite 5A was used to separate N_2, O_2, NO, CO, and CH_4 and Chromosorb 102 to analyze CO_2 and N_2O.

c. Catalyst Characterization

Perturbed angular correlation (PAC) technique. An experimental arrangement of four CsF coplanar detectors at 90° for a fast–fast coincidence system was used. The equipment resolution time was 0.8 ns. The time differential observation of the perturbed angular correlation of γ rays emitted from radioactive ^{111}In allows us to characterize different In species by means of different hyperfine interactions characteristic of each In site present in the sample. The principle of the application of PAC to In compounds consists of determining the hyperfine interaction between the nuclear quadrupole moment of the intermediate level of the γ–γ cascade (171–245 keV) of the nuclear probe ($^{111}In \rightarrow {}^{111}Cd$) and the EFG produced by all extranuclear charges, i.e., the electronic charges of the same atom plus the ionic charges of the lattice (mainly the first neighborhood of the probe).

The method relies on the fact that, due to the conservation of angular momentum, the direction of emission of a particle (photon) in a nuclear decay is strictly correlated with the orientation of the nuclear spin. Since nuclear spins are normally randomly oriented, the radiation pattern of a radioactive sample is generally isotropic. An anisotropic pattern can be obtained only if one has a set of atoms whose nuclear spins are equally oriented. This can be achieved by cooling the sample to very low temperatures or applying a strong magnetic field (as in NMR). In PAC technique, the detection in coincidence of two successive γ rays from a γ–γ nuclear cascade is used to obtain an anisotropic pattern. In effect, the observation of the first γ ray of the cascade determines the preferential direction of the nuclear spin, so that the detection of the second γ ray in coincidence with the first shows an angular correlation. This angular correlation can be perturbed via the interaction of nuclear quadrupole moment of the intermediate level of the cascade with the extranuclear field gradient, provided the nucleus remains in the intermediate excited state for a sufficiently long time (several nanoseconds typically).

The EFG is a second range tensor and hence it also contains information about the symmetry of the environment of the ^{111}In-probe atoms. These results from the charge density distribution reflect the nature of the chemical bonds. Inequivalent probe sites in the unit cell or inequivalent sites due to the coexistence of several phases in the sample lead to a superimposition of "perturbation functions" $A_{22}G_{22}(t)$, which are fitted with different weights to obtain characteristic parameters (quadrupole frequency ω_Q, asymmetry parameter η) for each weighted (through its relative concentration f) probe site [3].

When a set of probes have very similar near-neighborhoods, a finite frequency distribution (δ) around a mean "precession frequency" due to inhomogeneities can be obtained. If the EFG tensor deviates from axial symmetry, then the intensities and precession frequencies are also functions of the asymmetry parameter. In our case, these "inhomogeneities" can also be produced by ^{111}In probes located in very small crystallites. For low dimensionalities the defects are increased and then the probe sites have high inhomogeneities.

Temperature-programmed reduction and X-ray diffraction. X-Ray diffraction analysis was performed with a Shimadzu XD-D1 instrument with monochromator and Cu$K\alpha$ radiation with a scanning rate of 1° per minute.

Temperature-programmed reduction experiments were carried out in an Okhura TS-2002 instrument. Typically, 300 mg of the solid was pretreated in an argon atmosphere by heating up to 500°C at 5°C/min and holding the final temperature for 4 h. Afterward, the TPR was performed using 2% hydrogen in argon, 40 cm^3/min, with a heating rate of 10°C/min, from 25 to 700°C.

3. RESULTS AND DISCUSSION

a. PAC Spectra of Impregnated Samples (S1): Effect of Different in Loadings

Figure 1 shows PAC spectra taken at 500°C in air and their Fourier transforms for impregnated samples with different In loadings (0.6, 2, 3, and 4 wt%). Previously, these samples were heated at 500°C in an oxygen atmosphere (standard procedure). In Table 1, the corresponding hyperfine parameters f, ω_Q, η, and δ are shown. The PAC spectra for low indium concentrations (0.6 and 2.0 wt%) show a similar behavior. In the two cases we find that there is no unique environment for the indium and a distributed interaction (I_d) is observed. On the other hand, for a concentration of 4 wt% indium, we observed a notorious change in the PAC spectrum. In effect, the spectrum of this sample after thermal treatment at 500°C for 12 h presents two well-defined interactions (I_1, I_2) which correspond to those found for indium sesquioxide, which has been extensively studied with this technique (17–19). The sample with 3% In shows intermediate behavior. Both In_2O_3 interactions (I_1, I_2) and an interaction similar to that found in the lower-indium samples (I_d) are observed.

To study the process of indium sesquioxide formation PAC spectra at different calcination times were recorded at 500°C. Figure 2 shows PAC spectra of impregnated In(4 wt%)/H-ZSM5 calcined at 500°C for 3, 8, and 14 h. In Table 2 the fitted hyperfine parameters are displayed. After a 3-h thermal treatment the spectrum presents three interactions. Two of them are the well-defined indium sesquioxide signals (I_1, I_2); the third one is highly distributed and similar to the one observed in the low-indium loaded samples (I_d). After an 8-h thermal treatment, it is observed that the first two interactions become more intense whereas the third one decreases at the expense of the other two, while its distribution also decreases. If the thermal treatment is maintained for 6 additional hours, it can be observed that the interaction I_d completely disappears and that only the signals corresponding to indium oxide remain. Different

TABLE 1

Fitted Values of the Parameters Characterizing the Observed Interactions in the PAC Spectra of Fig. 1

S1—In (wt%)	f (%)	ω_Q (MHz)	η	δ (%)	Label
0.6	100	122(3)[a]	0	46(9)	I_d
2	100	128(3)	1	38(2)	I_d
3	25(4)	120(1)	0.69(1)	0.1(1)	I_1
	7(4)	157(2)	0.1(1)	1(1)	I_2
	68(5)	131(4)	0.56(6)	18(2)	I_d
4	76(5)	116.8(3)	0.71(1)	1.0(3)	I_1
	24(2)	152(1)	0.11(2)	0.2(3)	I_2

[a] The error in the last digit is indicated in parentheses.

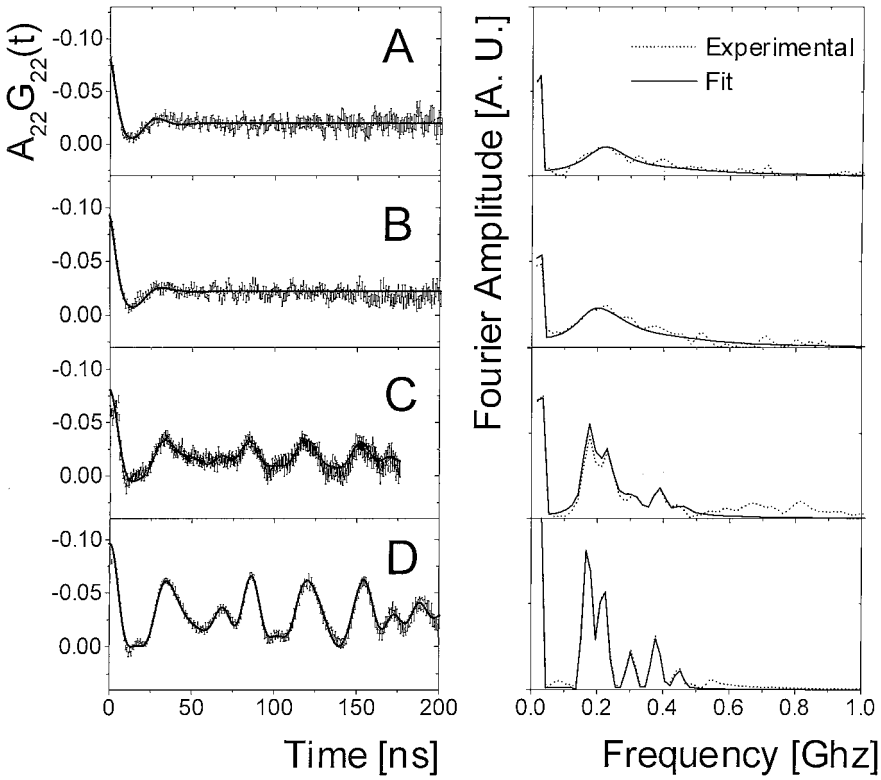

FIG. 1. PAC spectra and their Fourier transforms taken at 500°C of impregnated samples (S1) calcined 12 h at 500°C with 0.6 wt% indium (A), 2 wt% indium (B), 3 wt% indium (C), and 4 wt% indium (D).

from what happens with PAC, the X rays do not show the appearance of any structure formed by the indium in the indium zeolite spectrum treated at 500°C. The two main peaks of indium oxide [$d = 2.9$ Å and $d = 2.74$ Å (20)] are not observed.

b. PAC Spectra of In(4%)/H-ZSM5-Impregnated Sample (S1): Effect of Pretreatment

It is already known that different pretreatment atmospheres and temperatures originate different indium

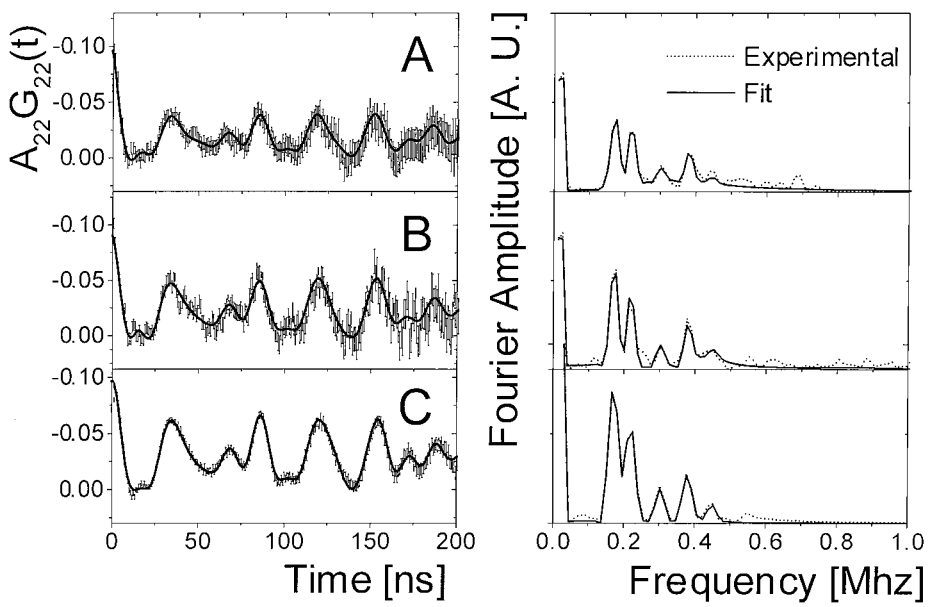

FIG. 2. PAC spectra and their Fourier transforms taken at 500°C of sample impregnated with 4 wt% indium (S1) calcined 3 h at 500°C (A), 8 h at 500°C (B), and 12 h at 500°C (C).

TABLE 2

Fitted Values of the Parameters Characterizing the Observed Interactions in the PAC Spectra of Fig. 2

Sample	f (%)	ω_Q (MHz)	η	δ (%)	Label
S1 (3 h at 500°C)	39(13)[a]	119.1(3)	0.71(1)	0.3(3)	I_1
	12(4)	154(1)	0	1(1)	I_2
	49(5)	134(14)	1	50(10)	I_d
S1 (8 h at 500°C)	55(11)	117.6(3)	0.71(1)	0.5(3)	I_1
	20(3)	153(1)	0.1(1)	1(1)	I_2
	25(3)	242(13)	1	15(5)	I_d
S1 (14 h at 500°C)	76(5)	116.8(3)	0.71(1)	1.0(3)	I_1
	24(2)	152(1)	0.11(2)	0.2(3)	I_2

[a] The error in the last digit is indicated in parentheses.

TABLE 3

Fitted Values of the Parameters Characterizing the Observed Interactions in the PAC Spectra of Fig. 3

Sample	f (%)	ω_Q (MHz)	η	δ (%)	Label
S1 (treatment A)	39(7)[a]	119(1)	0.69(2)	1(1)	I_1
	13(5)	156(2)	0.19(4)	6(2)	I_2
	47(5)	203(3)	0.36(3)	8(2)	I_3
S1 (treatment B)	100	234(2)	0.60(2)	4(2)	I_4
S1 (treatment C)	66(10)	114(4)	1	40(8)	I_d
	34(15)	211(3)	0.79(2)	8(2)	I'_3

[a] The error in the last digit is indicated in parentheses.

species supported on H-ZSM5 matrix (21). For example, it has been reported that high-temperature treatment (higher than 600°C) in oxygen favors the reaction between In_2O_3 and zeolite protonic sites to form $(InO)^+Z^-$ sites (22, 23). Reductive treatments followed by reoxidation also result in the formation of these sites (24). To gain insight on this aspect, PAC spectra of impregnated In(4%)/H-ZSM5 were recorded after different treatments (A, B, C). In Fig. 3, PAC spectra and Fourier transforms are depicted, and Table 3 shows the corresponding fitted hyperfine parameters.

In Fig. 3A, PAC spectra taken at 500°C of impregnated In(4%)/H-ZSM5 calcined at 750°C (treatment A) show three different signals: the first two previously assigned to In_2O_3 (I_1, I_2) and a new one (I_3) with a concentration of ca. 47%. This new signal should be assigned to $(InO)^+Z^-$ species formed, as said above, by the incomplete reaction between indium sesquioxide and zeolitic protons. Figure 3B shows PAC spectra taken at 500°C under hydrogen flow after treatment B. If compared with Fig. 3A, a totally different spectrum characterized by a new interaction (I_4) is observed. This interaction should be attributed to In^+Z^- species. In fact, it has been reported that under reducing conditions the overall transformation $In_2O_3 + 2H^+Z^- + 2H_2 = 2In^+Z^- + 3H_2O$ readily takes place (24). After reoxidation in oxygen at 500°C, the recorded PAC spectrum at 500°C changes again (Fig. 3C) showing two signals: one of them (I'_3) very similar (not exactly the same) to that above assigned to $(InO)^+Z^-$ species, and another distributed signal (I_d) with 60% concentration.

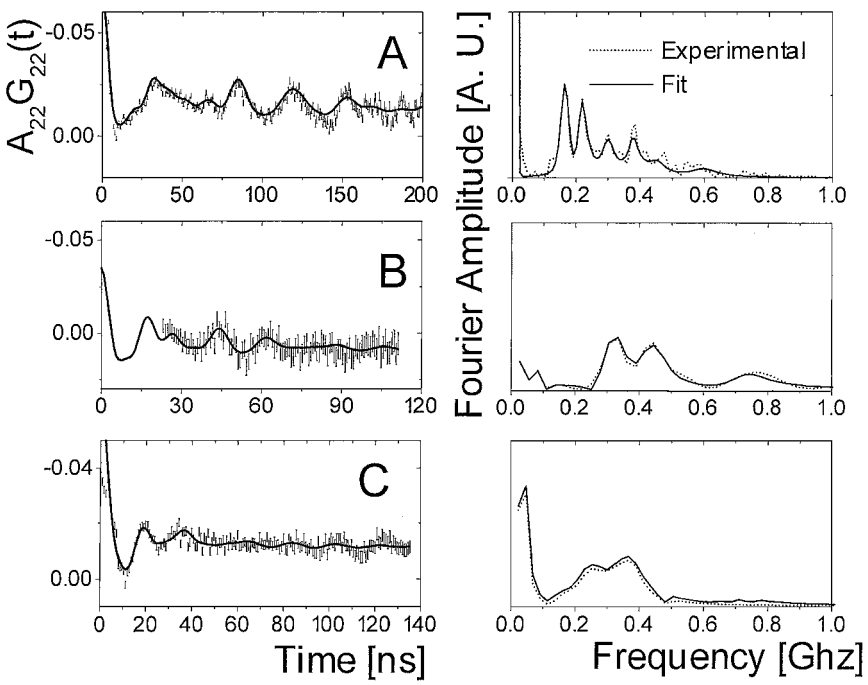

FIG. 3. PAC spectra and their Fourier transforms taken at 500°C of sample impregnated with 4 wt% indium (S1) after treatment A (A), after treatment B (and taken in H_2 atmosphere), and after treatment C (C).

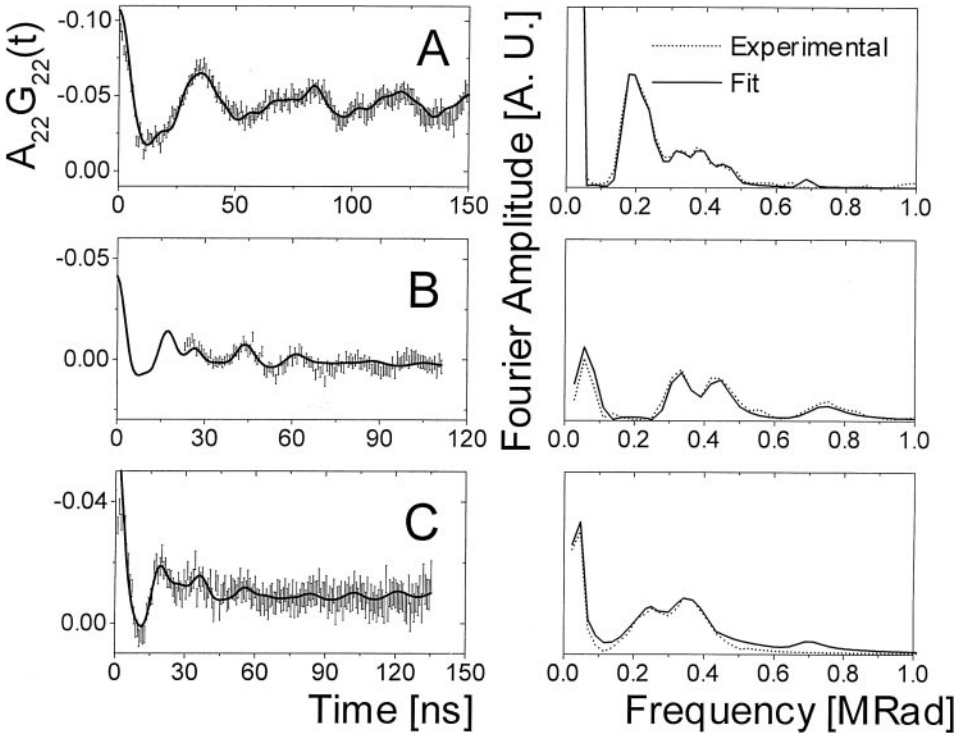

FIG. 4. PAC spectra and their Fourier transforms taken at 500°C of In-exchanged sample (S2) after standard calcination procedure (A), after treatment B (and taken in H_2 atmosphere) (B), and after treatment C (C).

Note that the last distributed signal has hyperfine parameters different from those observed in the low-loaded In samples.

c. PAC Spectra of In-Exchanged NH_4-ZSM5 (S2)

In Fig. 4 and Table 4 are shown PAC results of In-exchanged NH_4-ZSM5 (S2) spectra taken at 500°C. Figure 4A shows that after the standard calcination procedure, the PAC spectrum consists of four different interactions. Two of them (I_1, I_2) correspond to In_2O_3; a third signal (I_3') has the same characteristics of the signal assigned to $(InO)^+Z^-$ in Fig. 3B; and the fourth signal (I_d) similar to the unidentified distributed interaction also observed in Fig. 3B. After reduction in hydrogen at 500°C (Fig. 4B) and reoxidation in O_2 at 500°C (Fig. 4C) the observed spectra are the same as those observed in Figs. 3B and 3C for the impregnated sample with the same treatments (B and C). All the above assignments are summarized in Table 5 together with the corresponding calculated concentrations.

TABLE 4

Fitted Values of the Parameters Characterizing the Observed Interactions in the PAC Spectra of Fig. 4

Sample	f (%)	ω_Q (MHz)	η	δ (%)	Label
S2	58(3)[a]	119(2)	0.74(2)	4(4)	I_1
	19(2)	160(2)	0	2(2)	I_2
	14(3)	198(9)	0.7(1)	6(5)	I_3
	9(2)	135(4)	0.7(1)	4(4)	I_d
S2 (treatment B)	100	235(4)	0.60(3)	4(1)	I_4
S2 (treatment C)	71(10)	131(5)	1	30(6)	I_d
	29(15)	211(3)	0.83(2)	5(2)	I_3'

[a] The error in the last digit is indicated in parentheses.

d. Temperature-Programmed Reduction Results

TPR experiments were carried out to confirm some of the assignments shown in Table 5. Figure 5 depicts TPR of impregnated In(2%)/H-ZSM5, In(4%)/H-ZSM5, and In(12%)/H-ZSM5. The last sample was not characterized with the PAC technique, and was prepared with the aim of observing the TPR signal of the bulk In_2O_3 that does not interact with protonic sites (note that there is a considerable In excess). A reduction peak centered at 300°C which would correspond to the reduction of the In species having I_d interaction can be observed in the TPR of the In(2%) sample (a). The TPR of the sample with In(4%) (b) shows two nonresolved peaks, which would correspond to the reduction of the In_2O_3 crystals having I_1 and I_2 hyperfine interactions. The two-step reduction may be due to the presence of crystals of different size. It should be pointed out that the relatively low-temperature reduction of these In species is

TABLE 5

Summary of Hyperfine Interactions

Treatment	Relative population of hyperfine interactions					
	I_d	I_1	I_2	I_3	I_3'	I_4
i. Relative population of hyperfine interactions for In(4%)-impregnated catalyst (S1) with different treatments						
Standard		76(5)	24(2)			
A		39(7)	13(5)	47(5)		
B						100
C	60(10)				31(15)	
In_2O_3		74(3)	20(2)			
ii. Relative population of hyperfine interactions for In-exchanged catalyst (S2) with different treatments						
Standard	9(2)	58(3)	19(2)		14(3)	
B						100
C	63(10)				26(10)	
iii. Interaction assignments						
Label:	I_d	I_1	I_2	I_3	I_3'	I_4
Interaction assignment:	In with non-unique environment	In_2O_3 (site C)	In_2O_3 (site D)	$(InO)^+Z^-$	$(InO)^+Z^-$	In^+Z^-

due to the interaction with the protons on the zeolite surface through the reaction $In_2O_3 + 2H^+Z^- + 2H_2 = 2In^+Z^- + 3H_2O$ (24).

After TPR of the In(2%) sample, it was reoxidized at 500°C, and a new TPR was carried out (c). It can be observed that the TPR peak shifted to lower temperature, and would be assigned to the reduction of $(InO)^+Z^-$ species generated by oxidation of the In^+Z^- sites.

TPR of the sample loaded with 12% In (a large In excess) shows two peaks. The first is due to reduction of the portion of In_2O_3 that can interact with proton sites, and the high-temperature peak is characteristic of the reduction of bulk In_2O_3.

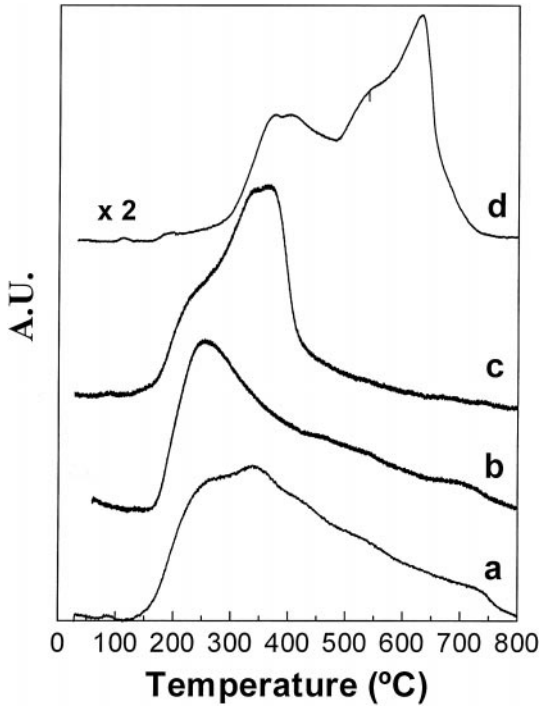

FIG. 5. TPR profiles of In-impregnated samples (In/H/ZSM5). (a) In(2%) after standard calcination procedure (12 h at 500°C). (b) In(2%) after former TPR and reoxidation at 500°C. (c) In(4%) after standard calcination procedure. (d) In(12%) after standard calcination procedure.

e. Reaction Results

Abundant data are available in the literature for the NO SCR reaction with methane in the presence of excess oxygen using In-based catalysts (12–14, 25–28). The reaction results in Table 6 are provided to help the reader better understand the role of In species characterized in the

TABLE 6

Comparative Results for the NO Selective Reduction with CH_4 over In/H/ZSM5[a]

Catalyst	Treatment	C_{NO} (350°C)	C_{CH_4} (350°C)	$C_{NO\ max}$[b]	T_{max}[c] (°C)
In(0.6%) S1	Standard	2	1	26	500
In(0.6%) S1	C	32	19	84	450
In(2%) S1	Standard	0	0	31	550
In(2%) S1	C	44	37	88	450
In(4%) S1	Standard	0	0	21	450
In(4%) S1	C	28	25	91	450
In(4%) S1	A	36	19	93	450
In(1.3%) S2	Standard	15	10	89	450
In(1.3%) S2	C	20	12	90	450

[a] Reaction conditions: 0.5 g of catalyst, 1000 ppm of NO, 1000 ppm of CH_4, 10% of O_2 in He. Total flow rate = 50 cm^3.

[b] NO maximum conversion.

[c] Temperature of NO maximum conversion.

previous section. Conversions of NO and CH_4 for the catalysts studied in this work are summarized. Since it is well known that NO-versus-temperature curves usually have a volcano shape, the maximum NO conversions attained are included in the table together with lower-temperature conversions (350°C).

Since different behaviors were observed, Fig. 6A shows a comparison of SCR reaction selectivities (NO conversion/CH_4 conversion) for the In(4%)-impregnated catalyst with different treatments (A and C). On the other hand, Figure 6B shows the results of the $CH_4 + O_2$ reaction for the same solids. From these reaction results, the following interesting points arise:

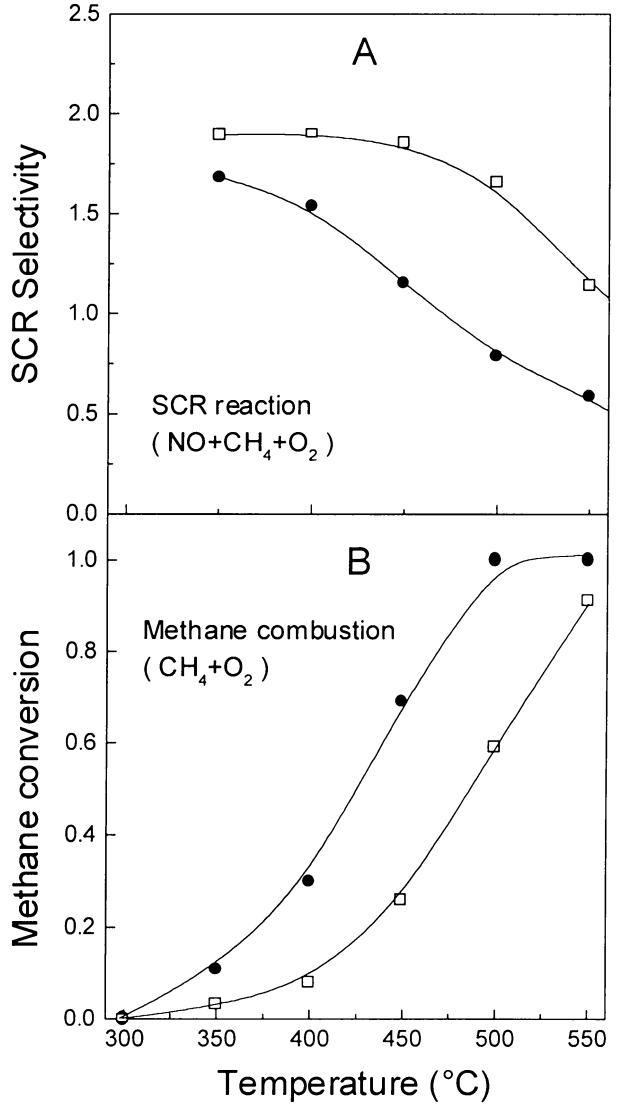

FIG. 6. Effect of pretreatment on SCR selectivity (NO conversion/CH_4 conversion) (A) and on methane combustion reaction (B). In(4%)/HZM5-impregnated catalyst. □, Treatment A (750°C for 2 h). ●, Treatment C (reduction for 2 h in H_2 at 500°C followed by reoxidation for 2 h in O_2 at the same temperature). Reaction conditions: 0.5 g of catalyst, 1000 ppm of NO, 1000 ppm of CH_4, 10% O_2 in He. Total flow rate = 50 cm^3.

While impregnated samples after the standard calcination procedure (12 h at 500°C) have poor activity, the ion-exchanged NH_4-ZSM5 sample after the same pretreatment is active for the NO SCR reaction.

Both after treatment A (750°C, 2 h) and after treatment C (H_2, 500°C followed by O_2, 500°C), the In(4%)-impregnated sample is active for the reaction under study.

All active samples contain species I_3 or I_3'.

Selectivity (NO_x conversion/CH_4 conversion) is higher for the impregnated sample after treatment A if compared with the same sample after treatment C.

The In(4%)-impregnated sample, activated by treatment C, shows an unidentified distributed signal I_d. This signal is absent after treatment A.

The lack of selectivity is related to the activity for the CH_4 combustion reaction (see Figs. 6A and 6B).

f. Role of the Different In Species in the SCR of NO with CH_4

PAC characterization of In/H-ZSM5 shows that different types of indium species are present, the distribution and relative concentrations being highly sensitive to preparation and treatment procedures. Moreover, while indium ion exchange yields an active catalyst for the SCR reaction, the wet impregnation method results in rather inactive solids (in both cases after the standard calcination procedure). This difference can be explained by taking into account the In species present in the solution during catalyst preparation.

It is generally accepted that it is difficult to exchange trivalent ions into ZSM5 (29). Because the lattice is relatively hydrophobic and the anionic field is weak, precipitation of hydroxides and exchange of metal hydroxide ions such as $[M(OH)_2]^+$ would be possible (21). At low concentrations hydroxide ions predominate, but at higher concentrations, polynuclear cations $In[(OH)_2In]_n^{(3+n)}$ are formed (30). The solution of $InCl_3$ used during the ion-exchange procedure has a relatively low concentration (2×10^{-3} mol/liter), and its volume remains constant under the reflux conditions used. For the impregnation method, the initial concentration is ca. 10 times higher than for the ion exchange, and the water is evaporated until an almost dry paste is obtained. Thus, it is reasonable to think that $In(OH)^{2+}$ and $In(OH)_2^+$ ionic species prevail during the ion exchange, and that polynuclear $In[(OH)_2In]_n^{(3+n)}$ species formation is favored during the wet impregnation procedure. While indium hydroxide species can diffuse into the ZSM5 channels during ion exchange, voluminous polynuclear cations are deposited onto the ZSM5 external surface during wet impregnation procedure, thus explaining the different properties of the solids obtained.

After calcination (500°C) of impregnated samples, In-containing polynuclear cations are probably dehydrated, forming small In oxide particles deposited on the zeolite external surface. In the PAC spectra corresponding to the impregnated samples with low indium concentrations (0.6 and 2 wt%), a distributed quadrupolar frequency appears whereas the indium sesquioxide structure is not observed. The structures that the indium would be forming in this case could be of the sesquioxide type but very dispersed and/or of very low dimension. In effect, if we take into account that the sesquioxide unit cell is 10 Å, the microcrystals should be of a couple of unit cells in diameter. In this situation, there should be indium atoms on the surface experiencing electric field gradients different from those of the oxide and probably different from each other. This set of indium sites with different electric field gradients would have, for the PAC spectrum, an appreciable distribution for their characteristic hyperfine interaction.

For the H-ZSM5 zeolite with 4% indium, well-defined hyperfine parameters are obtained, corresponding to the In_2O_3 formed on the zeolite external surface. PAC spectra taken at different calcination times clearly show that a very disperse In oxide phase is first formed. These small particles are the precursors of well-defined indium sesquioxide crystals formed after 12 h of calcination at 500°C. This phenomenon is not observed for the low indium-loaded samples probably because the small In particles cannot interact among them.

Impregnated samples calcined at 500°C have low activity for the SCR of NO with methane, which indicates that neither well-dispersed In oxide phase nor In sesquioxide crystals are active species for the said reaction.

Both treatment A (750°C in oxygen) and treatment C (reduction at 500°C followed by reoxidation) result in an active catalyst, and in both cases similar hyperfine interactions are observed (I_3 and I_3'). Since there is agreement in the literature on the structure of the active sites (12–14) and their mechanism of formation (22, 23), I_3 and I_3' signals should be assigned to $(InO)^+Z^-$ species with slightly different environments. This interaction is also present in In-exchanged NH_4-ZSM5. As mentioned above, the exchange solution would preferentially contain $In(OH)_2^+$ species, which could be exchanged in the $NH_4{}^+Z^-$ zeolitic sites. During calcination at 500°C dehydration takes place [$In(OH)_2{}^+Z^- = (InO)^+Z^- + H_2O$], thus forming active sites. However, PAC spectra show that only a fraction of the In is in the form of $(InO)^+$, the remaining fraction being mainly In_2O_3. This suggests that in the exchange solution a mixture of hydroxide and polynuclear cations is present.

Reaction results indicate that the In(4%)-impregnated catalyst is more selective after treatment A than the same catalyst after treatment C. While after treatment A the observed In species are $(InO)^+Z^-$ and In_2O_3, after treatment C the observed In species are $(InO)^+Z^-$ and the dispersed In phase characterized by the I_d hyperfine interaction. This suggests that In_2O_3 well-defined crystals do not participate in the reaction and the dispersed In species (small crystals) participate mainly in the methane combustion reaction ($CH_4 + 2O_2 = CO_2 + 2H_2O$), thus lowering the selectivity of the overall SCR reaction.

4. CONCLUSIONS

The distribution and type of indium species formed on the H-ZSM5 support are highly sensitive to the preparation and pretreatment methods used. The wet impregnation method followed by calcination at 500°C results in low-activity catalysts. However, treatment A in oxygen at 750°C or treatment C in hydrogen at 500°C followed by reoxidation at the same temperature activated the impregnated catalysts. The ion exchange method followed by calcination at 500°C also gave an active catalyst.

All the active solids show similar hyperfine interactions (I_3 and I_3') attributed to the presence of $(InO)^+Z^-$ species.

Both In_2O_3 crystals (hyperfine interactions I_1 and I_2) and highly dispersed noncrystalline indium oxide species (hyperfine interaction I_d) are inactive for the SCR of NO with methane. The latter species, however, are active for methane combustion with oxygen. These species are not chemically bonded to the zeolite structure.

The PAC technique, combined with TPR and activity measurements, is a powerful tool for the identification and quantification of surface In species.

ACKNOWLEDGMENTS

The authors acknowledge Ing. J. Runco's technical assistance in the PAC experimental setup. This work was partially supported by CICpBA. The authors are also grateful to CONICET and UNL (CAI+D '96 Program). Thanks are extended to Elsa Grimaldi for editing the English manuscript.

REFERENCES

1. Requejo, F. G., and Bibiloni, A. G., *Phys. Status Solidi. A* **148**, 497 (1995).
2. Requejo, F. G., and Bibiloni, A. G., *Langmuir* **12**(1), 51 (1996).
3. Frauenfelder, H., and Steffen, R. M., *in* "Alpha-, Beta- and Gamma-Ray Spectroscopy" (K. Siegbahn, Ed.), Vol. 2, p. 997. North-Holland, Amsterdam, 1968.
4. Vogdt, C., Butz, T., Lerf, A., and Knözinger, H., *J. Catal.* **116**, 31 (1989).
5. Marchi, A. J., Lede, E. J., Requejo, F. G., Rentería, M., Irusta, S., Lombardo, E. A., and Miró, E. E., *Catal. Lett.* **48**, 47 (1997).
6. Irusta, S., Requejo, F. G., Lombardo, E. A., and Miró, E. E., *Lat. Am. Appl. Res.* **24**, 187 (1994).
7. Li, Y., and Armor, J. N., U.S. Patent 5,149,512 (1992).
8. Li, Y., and Armor, J. N., *Appl. Catal. B* **1**, L31 (1992).
9. Yogo, K., Ihara, M., Terasaki, I., and Kikuchi, E., *Chem. Lett.*, 229 (1993).
10. Kikuchi, E., and Yogo, K., Presented at the International Forum on Environmental Catalysis '93, Tokyo, Japan, Feb. 4–5, 1993.
11. Li, Y., and Armor, J. N., *J. Catal.* **145**, 1 (1994).
12. Kikuchi, E., and Yogo, K., *Catal. Today* **22**, 73 (1994).

13. Kikuchi, E., Ogura, M., Aratani, N., Sugiura, Y., Hiromoto, S., and Yogo, K., *Catal. Today* **27**, 35 (1996).
14. Ogura, M., Hayashi, M., and Kikuchi, E., *Catal. Today* **42**, 159 (1998).
15. Ramallo López, J. M., Requejo, F. G., Rentería, M., Bibiloni, A. G., and Miró, E. E., *Hyp. Int.*, in press.
16. Vassallo, J., Miró, E. E., and Petunchi, J., *Appl. Catal. B* **7**, 65 (1995).
17. Desimoni, J., Bibiloni, A., Mendoza Zelis, L., Pasquevich, A., Sánchez, F., and López García, A., *Phys. Rev. B* **28**, 5739 (1983).
18. Bartos, A., Lieb, K. P., Pasquevich, A. F., and Uhrmacher, M., *Phys. Lett. A* **157**, 513 (1991).
19. Habenicht, S., Lupascu, D., Uhrmacher, M., Ziegeler, L., and Lieb, K. P., *Z. Phys. B* **101**, 187 (1996).
20. Prewitt, C. T., Shannon, R. D., Rogers, D. B., and Sleight, A. W., *Inorg. Chem.* **8**, 1985 (1969).
21. Zhou, X., Zhang, T., Xu, Z., and Lin, L., *J. Mol. Catal. A* **122**, 125 (1997).
22. Kikuchi, E., Ogura, M., Terasaki, I., and Goto, Y., *J. Catal.* **161**, 465 (1996).
23. Ogura, M., Ohsaki, T., and Kikuchi, E., *Microporous Mesoporous Mater.* **21**, 533 (1998).
24. Beyer, H. K., Mihályi, R. M., Minchev, Ch., Neinska, Y., and Kanazirev, V., *Microporous Mater.* **7**, 333 (1996).
25. Heinisch, R., Jahn, M., and Wawrzinek, K., *Chem. Eng. Technol.* **20**, 641 (1997).
26. Tabata, T., Kokitsu, M., and Okada, O., *Appl. Catal. B* **6**, 225 (1995).
27. Zhou, X., Zhang, T., Xu, Z., and Lin, L., *Catal. Lett.* **40**, 35 (1996).
28. Ogura, M., and Kikuchi, E., *Stud. Surf. Sci. Catal.* **101**, 671 (1996).
29. Kaliaguine, S., Lemay, G., Adnot, A., Burelle, S., Audet, R., Jean, G., and Sawichi, J. A., *Zeolites* **10**, 559 (1990).
30. Wade, K., and Banister, J. A., *in* "Comprehensive Inorganic Chemistry," Chap. 12. Pergamon Press, Elmsford, NY, 1973.